ISSN 1029-9599, Physical Mesomechanics, 2017, Vol. 20, No. 3, pp. 305–310. © Pleiades Publishing, Ltd., 2017.
Original Russian Text © A.A. Sokolov, A.M. Krivtsov, W.H. Müller, 2017, published in Fizicheskaya Mezomekhanika, 2017, Vol. 20, No. 3, pp. 63–68.

Localized Heat Perturbation in Harmonic 1D Crystals: Solutions for an Equation of Anomalous Heat Conduction

A. A. Sokolov[1]*, A. M. Krivtsov[1,2], and W. H. Müller[3]

[1] *Peter the Great Saint-Petersburg Polytechnic University, St.-Petersburg, 195251 Russia*
[2] *Institute of Problems of Mechanical Engineering, Russian Academy of Sciences, St. Petersburg, 199178 Russia*
[3] *Institute of Mechanics, Chair of Continuum Mechanics and Constitutive Theory, Technische Universität Berlin, Berlin, 10587 Germany*
** e-mail: sokolovalexey1@gmail.com*

Received February 14, 2017

Abstract—In this paper exact analytical solutions for the equation that describes anomalous heat propagation in a harmonic 1D lattices are obtained. Rectangular, triangular and sawtooth initial perturbations of the temperature field are considered. The solution for an initially rectangular temperature profile is investigated in detail. It is shown that the decay of the solution near the wavefront is proportional to $1/\sqrt{t}$. In the center of the perturbation zone the decay is proportional to $1/t$. Thus, the solution decays slower near the wavefront, leaving clearly visible peaks that can be detected experimentally.

DOI: 10.1134/S1029959917030067

Keywords: heat conduction, harmonic crystals, one dimensional crystals, localized excitations, anomalous heat conduction

1. INTRODUCTION

Nowadays the investigation of nonlinear thermomechanical processes in low-dimensional structures attracts high interest due to the rapid development of nanoelectronical devices based on materials with microstructure [1–4]. Achievements in nanotechnology allowed for an experimental proof of the wave nature and finite propagation velocity of thermal perturbations [5, 6]. The study of such phenomena can result in a universal theory of heat conduction, applicable both on micro- and macroscales.

The classical heat equation is a parabolic partial differential equation that describes the distribution of temperature in a given spatial region over time:

$$\dot{T} = \beta T'', \quad (1)$$

where T is the temperature, β is the thermal diffusivity, the dot $(\dot{})$ denotes differentiation with respect to t, and the prime $(\;)'$ denotes differentiation with respect to x. The classical heat equation is derived on the basis of Fourier's law [7, 8]:

$$q = -\kappa \nabla T, \quad (2)$$

where κ is the thermal conductivity, q is the heat flux, and T is temperature. Practice shows that Fourier's law is well applicable to the description of heat processes on the macroscale. However, Fourier's law predicts an infinite speed of signal propagation, which can be physically paradoxical. A study of microprocesses, when the characteristic length is proportional to several atomic bond lengths, requires more complicated models of heat transfer that account for a finite velocity of heat propagation. Significant deviations from Fourier's law occur in one-dimensional crystalline structures [9]. Recent experimental works of one-dimensional nanostructures reveal the dependence of thermal conductivity on the structure length [10]. Strong deviations from Fourier's law are experimentally shown for C and BN nanotubes [11]. Thermal anomalies for nanostructures can be used for designing promising devices such as thermal diodes [4].

The anomalous nature of heat processes for one-dimensional lattices is demonstrated analytically by Rieder et al. [12] who studied the problem of heat flow between two heat baths. Numerous results on anomalous heat transfer in low-dimensional systems are summarized by Lepri et al. [8]. In describing such processes, hyperbolic heat Eq. [13, 14]

$$\tau \ddot{T} + \dot{T} = \beta T'', \quad (3)$$

where τ is the relaxation time, provides an alternative to classic heat Eq. (1). Equation (3) describes the finite speed of temperature propagation. However, it still has serious difficulties in describing heat transfer in one-dimensional crystals since no unique relaxation time can be determined [15].

A promising approach for the description of unsteady heat processes in 1D crystals was presented elsewhere [16–18]. By using correlational analysis, the initial stochastic problem for individual particles is reduced to a deterministic problem for statistical characteristics of the crystal. Its solution gave continuum Eq. (7) describing anomalous heat transfer in 1D harmonic lattices [17]. In the present paper we will derive exact analytical solutions for this equation, in particular, for rectangular, triangular and sawtooth initial distribution. Such properties as decay and asymptotics of the wavefront will be investigated in detail by the example of a rectangular initial perturbation. These results can be used for the analysis of anomalous heat transfer in more complex systems, such as 1D crystals on the elastic substrate [19] and 2D and 3D crystals [20]. The understanding of anomalous heat conduction is of special importance for the analysis of the experimental data that are to be obtained in the nearest future due to the rapid development of nanotechnologies.

2. LOCALIZED HEAT PERTURBATIONS IN A HARMONIC CHAIN

The harmonic chain is a simple and effective model for investigating anomalous heat phenomena. According to the previous work [17], let us consider an infinite harmonic chain. Each particle with mass m is connected to its neighbor by Hookean springs with stiffness C. The equation of motion of the particles reads

$$\ddot{u}_k = \omega_e^2(u_{k-1} - 2u_k + u_{k+1}), \quad \omega_e \overset{\text{def}}{=} \sqrt{C/m}, \tag{4}$$

where u_k is the displacement of a particle with index k. The following initial conditions are considered:

$$u_k\,|_{t=0} = 0, \quad \dot{u}\,|_{t=0} = \sigma(x)\rho_k, \tag{5}$$

where ρ_k is the independent random variables with zero expectation and unit variance and σ is the variance of the initial particle velocity. The variance is a slowly changing function of the spatial coordinate $x = ka$, where a is the initial distance between neighboring particles. Such initial conditions can be realized by ultrafast heating, for example, with a laser [21]. Let us introduce the kinetic temperature T as

$$k_\text{B}T = m\langle \dot{u}_k\rangle^2, \tag{6}$$

where $\langle ...\rangle$ is the operator averaging over realizations and k_B is the Boltzmann constant. The continuum partial differential equation for the kinetic temperature was previously obtained [17]:

$$\ddot{T} + \dot{T}/t = c^2 T'', \tag{7}$$

where c is the speed of sound in a one-dimensional crystal. Equation (7) describes the time evolution of the spatial temperature distribution in the chain. The following initial conditions for Eq. (7) correspond to stochastic initial problem (5):

$$\dot{T}\,|_{t=0} = 0, \quad T\,|_{t=0} = T_0(x). \tag{8}$$

Problem (7), (8) can be solved in the integral form [17]:

$$T(t, x) = 1/\pi \int_{-t}^{t} T_0(x - c\tau)\Big/\sqrt{t^2 - \tau^2}\, \mathrm{d}\tau. \tag{9}$$

Equation (7) is a particular case of the Darboux equation [22]. This type equation was earlier studied in context with spherical averages for solutions of the 2D and 3D wave equation, though being unstudied in relation to heat conduction phenomena. Equation (7) looks similar to hyperbolic heat Eq. (3), but it has a variable coefficient. This feature is due to anomalous heat transfer in a one-dimensional chain. From the form of Eq. (7), it may appear that it has a singularity. However, it does not matter because the equation should be solved with initial conditions (8) that exclude a singularity. The absence of singularity is confirmed by general solution (9) and specific solutions that will be considered below.

This paper is dedicated to finding exact analytical solutions of Eq. (7) for cases when the initial thermal distribution function $T_0(x)$ is a localized function of coordinates x:

$$T_0(x) = \begin{cases} 0, & x < -l, \\ \Phi(x), & -l < x < l, \\ 0, & x > l, \end{cases} \tag{10}$$

where $\Phi(x)$ is an arbitrary function and l is the half width of localized perturbation. Such initial temperature distribution can be experimentally derived by superfast laser heating of a localized region of the chain.

3. RECTANGULAR PERTURBATION

3.1. Solution

Let us consider a rectangular initial temperature distribution

$$T_0(x) = A(\mathrm{H}(x + l) - \mathrm{H}(x - l)), \tag{11}$$

where $\mathrm{H}(x)$ is the Heaviside function

$$\mathrm{H}(x) = \begin{cases} 0, & x < 0, \\ 1, & x \geq 0, \end{cases} \tag{12}$$

A is the amplitude of the initial temperature distribution. A substitution of formula (11) into solution (9) gives

$$T(t, x) = \frac{A}{\pi}\int_{-t}^{t}\frac{\mathrm{H}(x+l)}{\sqrt{t^2-\tau^2}}\mathrm{d}\tau - \frac{A}{\pi}\int_{-t}^{t}\frac{\mathrm{H}(x-l)}{\sqrt{t^2-\tau^2}}\mathrm{d}\tau. \quad (13)$$

By substituting the earlier obtained solution for a single Heaviside initial impulse [17]

$$T(x,t) \overset{\text{def}}{=} T_S(x,t) = \begin{cases} 0, & x \le -ct, \\ \dfrac{A}{\pi}\left(\pi - \arccos\dfrac{x}{ct}\right), & -ct \le x \le ct, \\ A, & x \ge ct. \end{cases} \quad (14)$$

to (13), we obtain the solution of the given problem as a linear combination of these solutions. Solution for positive x:

$t \le \tau_0$:

$$T(x,t) = \begin{cases} 0, & l+ct \le x, \\ \dfrac{A}{\pi}\arccos\left(\dfrac{x-l}{ct}\right), & l-ct \le x \le l+ct, \\ A, & 0 \le x \le l-ct, \end{cases} \quad (15)$$

$t \ge \tau_0$:

$$T(x,t) = \begin{cases} 0, & ct+l \le x, \\ \dfrac{A}{\pi}\arccos\dfrac{x-l}{ct}, & ct-l \le x \le ct+l, \\ \dfrac{A}{\pi}\left(-\arccos\dfrac{x+l}{ct} + \arccos\dfrac{x-l}{ct}\right), & 0 \le x \le ct-l, \end{cases} \quad (16)$$

where $\tau_0 = l/c$. For negative x, the solution, being symmetric, can be solved as $T(x, t) = T(-x, t)$.

For comparison, we consider the same initial problem for the classical heat equation:

$$\dot{T} = \beta T''. \quad (17)$$

The solution for an initial Heaviside step temperature distribution has the form [23]

$$T(x,t) = 1/2\left(1 + \mathrm{erf}\left(x/\sqrt{4\beta t}\right)\right), \quad (18)$$

where erf (x) is the Gaussian error function. Then, the solution of initial problem (8), (11), (17) is

$$T(x,t) = \frac{1}{2}\mathrm{erf}\frac{x+l}{\sqrt{4\beta t}} - \frac{1}{2}\mathrm{erf}\frac{x-l}{\sqrt{4\beta t}}. \quad (19)$$

The time evolution plots are shown for the solution of anomalous heat equation (7) in Fig. 1a and Fourier equation (17) in Fig. 1b. Let us compare the two solutions. The Fourier solution has a peak at $x = 0$ which decays exponentially. In the case of anomalous heat conduction, the solution decays in the area near $x = 0$ more rapidly than near the wavefront, thus forming two peaks propagating in the positive and negative directions with coordinates $x = -l + ct$ and $x = l - ct$.

3.2. Decay Behavior

Let us consider the decay behavior of solution (16) at $x = 0$. We perform a series expansion of the solution

$$T(t,0) = \frac{A}{\pi}\left[\pi - 2\arccos\frac{l}{ct}\right] = 2\varepsilon + O(\varepsilon^3), \quad (20)$$

where $\varepsilon = l/(ct)$ is the small parameter.

Now we turn to the decay behavior of the peaks $x = l - ct$ and $x = -l + ct$. From formula (16) it follows that

$$T(t,-l+ct) = T(t,l-ct) = \frac{A}{\pi}\left[\pi - \arccos\left(\frac{2l}{ct} - 1\right)\right] = 2\sqrt{\varepsilon} + O(\varepsilon^{3/2}). \quad (21)$$

Summarizing the above, we derive

$$T(t,0) \overset{t\to\infty}{\sim} 2\varepsilon \sim \frac{1}{t}, \qquad T(t,-l+ct) = T(t,l-ct) \overset{t\to\infty}{\sim} 2\sqrt{\varepsilon} \sim \frac{1}{\sqrt{t}}. \quad (22)$$

Thus, the solution decays more faster in the area between wavefronts (proportional to $1/t$), than near the wavefront (proportional to $1/\sqrt{t}$). Thus, the peaks remain strongly pronounced even for long times.

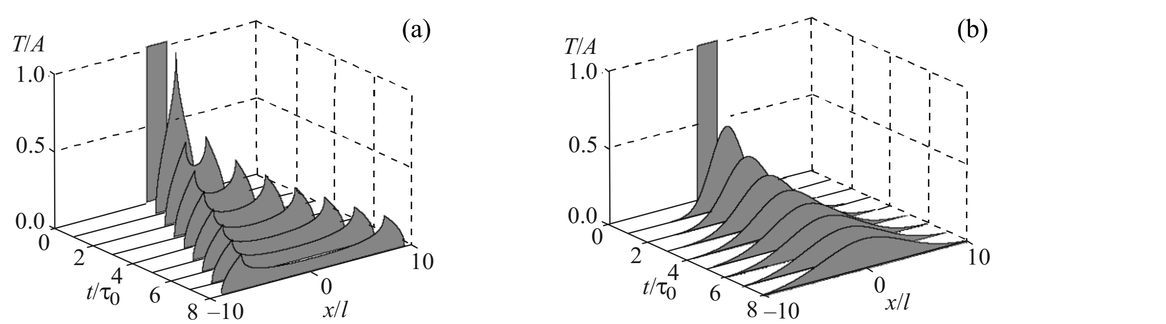

Fig. 1. Time evolution for solutions for a rectangular initial perturbation: anomalous (a) and classical heat conduction (b).

3.3. Envelope Curve for the Peaks

Solution has two peaks travelling in the positive and negative directions with speed c. As the solution is symmetric, we will consider only the peak with the coordinate $x = ct - l$. We shall consider the curve drawn by the peak of the solution as it travels in positive direction. By substituting $t = (x+l)/c$ into formula (21), we derive the expression for the envelope curve

$$T_{\text{env}}(x) = \frac{A}{\pi}\left[\pi - \arccos\left(\frac{2l}{x+l} - 1\right)\right]. \tag{23}$$

For any x, we have $T(x) \le T_{\text{env}}(|x|)$. The envelope curve is plotted in Fig. 2. Expression (23) decays as $1/\sqrt{x}$, which agrees with the statement that the solution decays as $1/\sqrt{t}$ near the wavefront (the wavefront travels with constant speed).

3.4. Asymptotic Behavior near the Wavefront

Let us consider solution (16) near the wavefront at long times t. Assume $\xi = (-x+ct)/l$. For $x \in [-l+ct, l+ct]$ we have

$$T(\xi, t) = \frac{A}{\pi}\arccos\left[1 - \frac{l}{ct}(\xi+1)\right] \overset{t\to\infty}{\sim} \frac{A}{\pi}\sqrt{\frac{2l}{ct}}\sqrt{\xi+1}, \tag{24}$$

where $(\xi+1)/(ct)$ is the small parameter used for expansion. For $x \in [l-ct, -l+ct]$ we acquire

$$T(\xi, t) = \frac{A}{\pi}\left(-\arccos\left[1 - \frac{l}{ct}(\xi-1)\right] + \arccos\left[1 - \frac{l}{ct}(\xi+1)\right]\right) \overset{t\to\infty}{\sim} \frac{A}{\pi}\sqrt{\frac{2l}{ct}}(\sqrt{\xi+1} - \sqrt{\xi-1}). \tag{25}$$

Functions (24) and (25) have the form

$$T = \frac{A}{\pi}\sqrt{\frac{2l}{ct}}F(\xi). \tag{26}$$

The relation means that the shape of the solution shrinks vertically with time, but it does not change horizontally. Dependences (16), (24), and (25) with the corresponding dimensionless time parameter $t/\tau_0 = 100$ are shown in Fig. 3. Asymptotic solutions (24) and (25) achieve peak values of T for $\xi = 1$, where $F(\xi) = \sqrt{2}$. The solution at this point remains continuous but not smooth (the derivative of the solution has a jump).

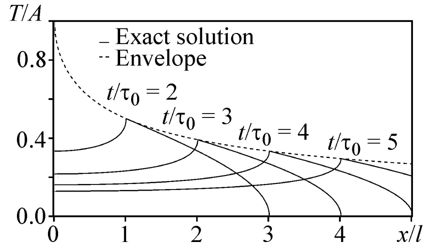

Fig. 2. Envelope curve for peaks of the solution.

4. TRIANGULAR PERTURBATION

In order to obtain the solution for a triangular initial function, we consider the following auxiliary problem where the initial temperature distribution is a linearly heated semispace:

$$T_0(x) = \begin{cases} 0, & x < 0, \\ Bx, & x \ge 0, \end{cases} \tag{27}$$

where $B = A/l$ is the constant of proportionality. A substitution of (27) into (9) gives the solution for $|x| < ct$

$$T(x, t) = Bx\left(\frac{1}{\pi}\arcsin x + \frac{1}{2}\right) + \frac{B}{\pi}\sqrt{t^2c^2 - x^2} \overset{\text{def}}{=} f(x), \tag{28}$$

and for $|x| > ct$ the initial temperature distribution is unaltered.

Now we pass to the problem on a triangular initial hear distribution, which can be expressed by the following piecewise function:

$$T_0(x) = \begin{cases} 0, \ x < -l, \\ (x+l)B, \ -l \le x < 0, \\ (-x+l)B, \ 0 \le x < l, \\ 0, \ x \ge l. \end{cases} \tag{29}$$

The solution for the initial temperature distribution (29) will be a linear combination of solutions for the linearly heated semispace. Denote solution (28) by T_L. The solution for initial distribution (29) will then be as follows:

$$T(t,x) = T_L(t, x-l) + T_L(t, x+l) - 2T_L(t, x). \tag{30}$$

The solution is symmetric: $T(x, t) = -T(x, t)$. The part corresponding to positive x has the following piecewise form:

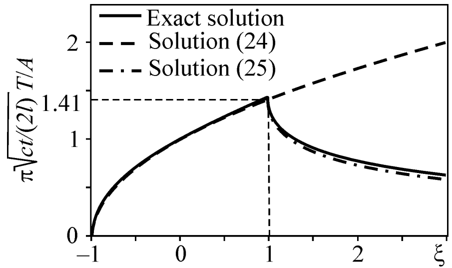

Fig. 3. Exact and approximate solutions for rectangular initial temperature distribution.

$t \le \tau_0/2$:

$$T(t,x) = \begin{cases} f(x+l) - 2f(x), \ 0 \le x \le ct, \\ (-x+l)B, \ ct \le x \le l-ct, \\ (-x+l)B + f(x+l), \ l-ct \le x \le l+ct, \\ 0, \ l+ct \le x, \end{cases} \quad (31)$$

$\tau_0/2 \le t \le \tau_0$: $T(t,x)$

$$= \begin{cases} (x+l)B - 2f(x), \ 0 \le x \le l-ct, \\ (x+l)B + f(x-l) - 2f(x), \ l-ct \le x \le ct, \\ (-x+l)B + f(x-l), \ ct \le x \le l+ct, \\ 0, \ l+ct \le x, \end{cases} \quad (32)$$

$t \ge \tau_0$: $T(t,x)$

$$= \begin{cases} f(x+l) + f(x-l) - 2f(x), \ 0 \le x \le -l+ct, \\ (x+l)B + f(x-l) - 2f(x), \ -l+ct \le x \le ct, \\ (-x+l)B + f(x-l), \ ct \le x \le l+ct, \\ 0, \ l+ct \le x. \end{cases} \quad (33)$$

The derived solution is represented graphically in Fig. 4. Unlike the solution for a rectangular initial distribution, which has a wavefront with vertical tangent and infinite derivative and a break of the temperature profile at the peak, the solution for a triangular distribution has a smooth beginning at the wavefront and smooth behavior at the peak.

5. SAWTOOTH PERTURBATION

We consider an initial heat distribution as a sawtooth distribution. It can be written in the following form:

$$T_0(x) = \begin{cases} 0, \ x \le -l, \\ x+l, \ -l \le x < 0, \\ 0, \ 0 \le x. \end{cases} \quad (34)$$

Initial conditions (34) can be written as linear combinations of a step function and linearly heated semispace. Then, the solution for sawtooth initial distribution (34) can be obtained from the corresponding combination of the solutions for a step initial distribution $T_S(x,t)$ and a linearly heated semispace initial distribution $T_L(x,t)$:

$$T(t,x) = T_L(x+l,t) + T_L(x,t) + T_S(x,t). \quad (35)$$

It has the following piecewise form:

$t \le \tau_0$: $T(x,t)$

$$= \begin{cases} 0, \ x \le -l-ct, \\ f(x+l), \ -l-ct \le x \le -l+ct, \\ Bx, \ -l+ct \le x \le -ct, \\ Bx - f(x) - \frac{A}{\pi}\arccos\frac{x}{ct}, \ -ct \le x \le ct, \\ 0, \ x > ct, \end{cases} \quad (36)$$

$t \ge \tau_0$: $T(x,t)$

$$= \begin{cases} 0, \ x \le -ct-l, \\ f(x+l), \ -ct-l \le x \le -ct, \\ f(x+l) - f(x) - \frac{A}{\pi}\arccos\frac{x}{ct}, \\ -ct \le x \le ct-l, \\ Bx - f(x) - \frac{A}{\pi}\arccos\frac{x}{ct}, \ ct-l \le x \le ct, \\ 0, \ ct \le x. \end{cases} \quad (37)$$

The solution is graphically illustrated in Fig. 5. The left wavefront has a smooth beginning and an infinite derivative at the peak. Contrary, the right wavefront has an infinite derivative at the beginning, smooth behavior at the peak, and a horizontal derivative at the peak.

6. CONCLUSION

The process of heat transfer in a 1D infinite harmonic chain was investigated. The evolution of localized initial distributions was considered. Solutions for the previously derived equation [17] describing anomalous heat conduction (7) were obtained. Exact analytical solutions for rectangular, triangular and sawtooth initial impulses were considered. It was shown that solutions for Eq. (7) unlike solutions for classical heat equation have a strongly

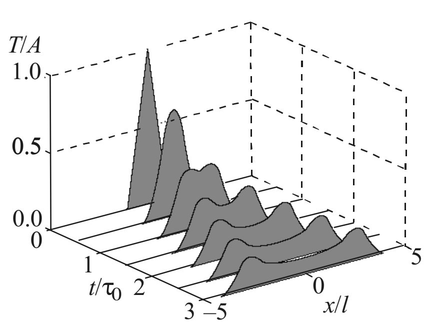

Fig. 4. Time evolution of the solution for a triangular initial perturbation.

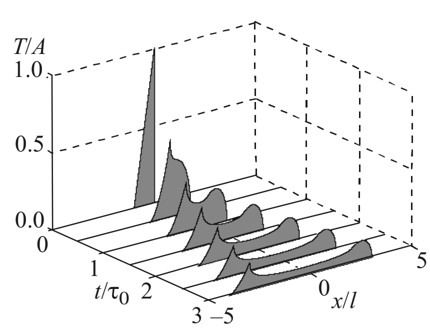

Fig. 5. Time evolution of the solution for a sawtooth initial perturbation.

pronounced wavefront. For the rectangular case, it was shown that the decay of the solution near the wavefront is proportional to $1/\sqrt{t}$ and near zero the decay is proportional to $1/t$. Thus, the solution decays slower near the wavefront, leaving clearly visible peaks. The shape of the wavefront is described by a function inversely proportional to the square root of time and has the form

$$T = \frac{A}{\pi}\sqrt{\frac{2l}{ct}}F(\xi).$$

The solution for a triangular initial temperature distribution has a smooth beginning at the wavefront and a smooth behavior at the peak. In the case of a sawtooth initial distribution, the solution is asymmetric: the left wavefront has a smooth beginning and an infinite derivative at the peak, and the right wavefront has an infinite derivative at the beginning, smooth behavior and horizontal tangent at the peak.

The obtained solutions demonstrate the wave behavior and power decay. This differs from the results obtained from the solutions of classic heat equation (1) (diffusive behavior, exponential decay) and hyperbolic heat equation (3) (wave behavior, exponential decay). Such properties of the obtained solutions can be used for analyzing the experimental data and choosing the right model for the description of the heat processes.

ACKNOWLEDGMENTS

The work was supported by the Russian Science Foundation (Grant No. 14-11-00599).

REFERENCES

1. Zhang, X., Luo, D., Cui, G., Wang, Y., and Huang, B., Construction of Logic Gate Based on Multi-Channel Carbon Nanotube Field-Effect Transistors, *Third Int. Conf. Intelligent Human-Machine Systems and Cybernetics, Aug 2011*, 2011, vol. 2, pp. 94–97.
2. Chen, Ch., Jin, T., Wei, L., Li, Y., Liu, X., Wang, Y., Zhang, L., Liao, Ch., Hu, N., Song, Ch., and Zhang, Y., High-Work-Function Metal/Carbon Nanotube/Low-Work-Function Metal Hybrid Junction Photovoltaic Device, *NPG Asia Mater.*, 2015, vol. 7, p. e220.
3. Goldstein, R.V. and Morozov, N.F., Mechanics of Deformation and Fracture of Nanomaterials and Nanotechnology, *Phys. Mesomech.*, 2007, vol. 10, no. 5–6, pp. 235–246.
4. Li, B., Wang, L., and Casati, G., Thermal Diode: Rectification of Heat Flux, *Phys. Rev. Lett.*, 2004, vol. 93, p. 184301.
5. Brown, E., Hao, L., Gallop, J.C., and Macfarlane, J.C., Ballistic Thermal and Electrical Conductance Measurements on Individual Multiwall Carbon Nanotubes, *Appl. Phys. Lett.*, 2005, vol. 87, no. 2, p. 023107.
6. Wang, Zh., Carter, J.A., Lagutchev, A., KanKoh, Y., Seong, N.-H., Cahill, D.G., and Dlott, D.D., Ultrafast Flash Thermal Conductance of Molecular Chains, *Science*, 2007, vol. 317, no. 5839, pp.787–790.
7. Cannon, J.R., *The One-Dimensional Heat Equation*, Cambridge: Cambridge University Press, 1984.
8. Lepri, S., Livi, R., and Politi, A., *Thermal Conduction in Classical Low-Dimensional Lattices*, Elsevier Science, 2002.
9. Hsiao, T.-K., Chang, H.-K., Liou, Sz-Ch., Chu, M.-W., Lee, Si-Ch., and Chang, Ch.-W., Observation of Room-Temperature Ballistic Thermal Conduction Persisting over 8.3 μm in SiGe Nanowires, *Nat. Nanotech.*, 2013, vol. 8, no. 7, pp. 534–538.
10. Zhang, H., Hua, Ch., Ding, D., and Minnich, A.J., Length Dependent Thermal Conductivity Measurements Yield Phonon Mean Free Path Spectra in Nanostructures, *Sci. Rep.*, 2015, vol. 5, p. 9121.
11. Chang, C.W., Okawa, D., Garcia, H., Majumdar, A., and Zettl, A., Breakdown of Fourier's Law in Nanotube Thermal Conductors, *Phys. Rev. Lett.*, 2008, vol. 101, p. 075903.
12. Rieder, Z., Lebowitz, J.L., and Lieb, E., Properties of a Harmonic Crystal in a Stationary Nonequilibrium State, *J. Math. Phys.*, 1967, vol. 8, no. 5. pp. 1073–1078.
13. Cattaneo, C., Sur une Forme de L'équation de la Chaleur Eliminant le Paradoxe d'une Propagation Instantanee, *Comptes Rendus*, 1958, vol. 247, pp. 431–433.
14. Vernotte, P., Les Paradoxes de la Theorie Continue de L'équation de la Chaleur, *Comptes Rendus*, 1958, vol. 246, pp. 3154–3155.
15. Gendelman, O.V. and Savin, A.V., Nonstationary Heat Conduction in One-Dimensional Chains with Conserved Momentum, *Phys. Rev. E*, 2010, vol. 81, p. 020103.
16. Krivtsov, A.M., Energy Oscillations in a One-Dimensional Crystal, *Doklady Physics*, 2014, vol. 59, no. 9, pp. 427–430.
17. Krivtsov, A.M., Heat Transfer in Infinite Harmonic One-Dimensional Crystals, *Doklady Physics*, 2015, vol. 60, no. 9, pp. 407–411.
18. Krivtsov, A.M., On Unsteady Heat Conduction in a Harmonic Crystal, *ArXiv preprint*, 2015, p. 1509.02506.
19. Babenkov, M.B., Krivtsov, A.M., and Tsvetkov, D.V., Energy Oscillations in a One-Dimensional Harmonic Crystal on an Elastic Substrate, *Phys. Mesomech.*, 2016, vol. 19, no. 3, pp. 282–290.
20. Kuzkin, V.A. and Krivtsov, A.M., An Analytical Description of Transient Thermal Processes in Harmonic Crystals, *Phys. Solid State*, 2017, vol. 59, no. 5, pp. 1051–1062.
21. Poletkin, K.V., Gurzadyan, G.G., Shang, J., and Kulish, V., Ultrafast Heat Transfer on Nanoscale in Thin Gold Films, *Appl. Phys. B*, 2012, vol. 107, no. 1, pp. 13–143.
22. Polyanin, A.D. and Nazaikinskii, V.E., *Handbook of Linear Partial Differential Equations for Engineers and Scientists*, Chapman and Hall/CRC, 2016.
23. Müller, I. and Müller, W.H., *Fundamentals of Thermodynamics and Applications with Historical Annotations and Many Citations from Avogadro to Zermelo*, Berlin: Springer, 2011.